Photoinduced Synthesis of Silver/polymer Nanocomposites

GABRIEL MUSTATEA[1, 2]*, IOAN CALINESCU[1], AUREL DIACON[1], LAVINIA BALAN[3]*

[1]University Politehnica of Bucharest, Faculty of Applied Chemistry and Materials Science, 149 Calea Victoriei, 010072, Bucharest, Romania

[2]National Research & Development Institute for Food Bioresources, 5 Ancuta Baneasa Str., 020323, Bucharest, Romania

[3]Institut de Science des Matériaux – IS2M, 15 Jean Starcky Street, 68057, Mulhouse, France

Direct photoreduction and photosensitization are powerful approaches for the in-situ synthesis in a polymer matrix. A silver–acrylate nanocomposite was prepared using a novel one-pot strategy involving simultaneous photoinduced reduction and free radical polymerization processes. The fabrication of metal nanocomposite was performed using an acrylate functionalized oligomer (polyethylene glycol 600 diacrylate) and a silver salt ($AgNO_3$). The formation of Ag-nanoparticles was followed by UV–Vis spectroscopy which shows a surface plasmon band at a wavelength range between 410 and 440 nm. Transmission electron microscopy revealed that the synthesized nanoparticles were spherical in shape with a diameter between 5 to 20 nm. The polymerization process was followed quantitatively by infrared spectroscopy, monitoring the disappearance of the characteristic bands for the acrylate double bonds (1410 cm^{-1}). The optimum conditions for obtaining the silver-polymer nanocomposites have been determined (silver precursor concentration, molar ratio silver precursor/photoinitiator, irradiation time and intensity). A reaction mechanism was proposed to explain the polymerization rate dependence on the silver cations content.

Keywords: Silver nanoparticles, photo polymerization, acrylate, nanocomposites

Silver nanoparticles represent an extremely interesting research field due to their optical, electronic and magnetic properties. A large number of methods have already been developed to produce materials containing silver nanostructures. A large number of methods for nanoparticles synthesis are reported; reactions in liquid, solid or gas phase have been examined in order to get the desired properties of the final product. In liquid phase the most important are: chemical or photochemical reduction, biosynthesis, laser ablation, high energy irradiation. Sometimes nanoparticles synthesis can be assisted by microwaves and ultrasounds [1-14].

Ag^0 is formed by the direct photoreduction of a silver source (silver salt or complex) or reduction of silver ions using photochemically generated intermediates, such as radicals (scheme 1) [15].

The incorporation of silver nanoparticles into a polymer matrix has gained a lot of interest due to the possibility of these materials to combine properties from both organic and inorganic systems [16]. Usually, two main methods are used for the realization of silver-polymer nanocomposites: in-situ and ex-situ methods [17-20]. The ex-situ methods consist in dispersing silver nanoparticles produced beforehand into a polymer matrix [16], but their size dispersion over a large scale is difficult to control, thus limiting the interest of the method [16,20]. The in-situ methods involve the generation of silver nanoparticles directly in the polymer matrix through chemical reduction of a cationic precursor that exhibits a better dispersion characteristic [21]. In-situ photochemical synthesis is one of the most powerful approaches to realize silver/polymer nanocomposites.

Experimental part

Polyethylene glycol 600 diacrylate (SR610) was purchased from Sartomer. Silver nitrate ($AgNO_3$) with a

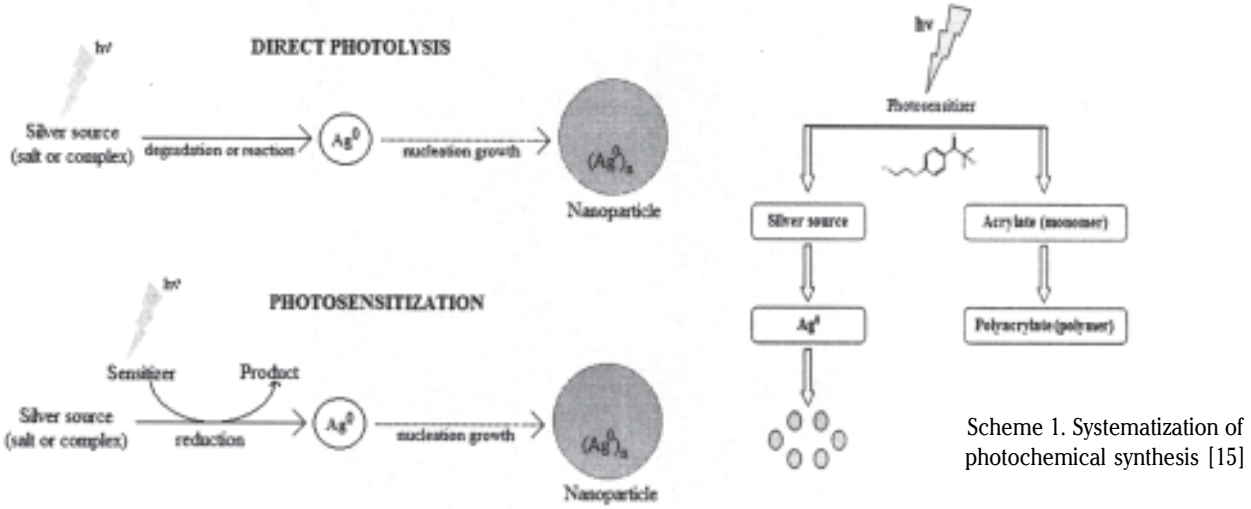

Scheme 1. Systematization of photochemical synthesis [15]

* email: mustatea_gaby@yahoo.com; Tel: +40720589957; lavinia.balan@uha.fr

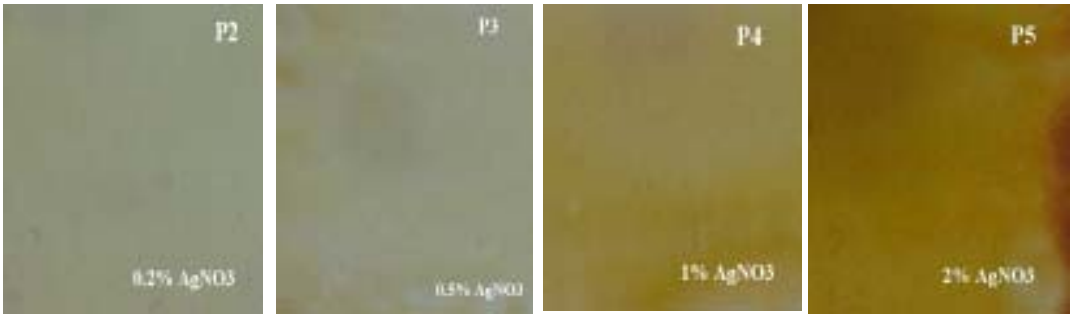

Fig. 1. Images of samples obtained using different concentrations of $AgNO_3$ and a constant concentration of photoinitiator

purity > 99% was purchased from Aldrich. The photoinitiator (UV sensitizer) 2-Hydroxy-4' -2-(hydroxy-ethoxy)-2-methyl-propiophenone (Irgacure 2959) was used as received.

The reactive oligomer and photoinitiator (0.5 wt % versus oligomer) were homogenized under stirring and different quantities of silver nitrate (0.2, 0.5, 1 and 2 wt %) were added. Synthesis of nanoparticles was performed by irradiation of the samples which were coated onto a glass substrate in the form of a film with a thickness of ~ 6 microns. In order to optimize the process, several factors (irradiation time, lamp intensity, amount of $AgNO_3$) were varied and their influence on the formation of nanoparticles was investigated.

The photopolymerization of the acrylate monomer was carried out under a Xe-Hg source (Lightning cure L8333 with a Hamamatsu L8253 Xe-Hg 100 W lamp). The polymerization was followed up in situ by Fourier transformed infrared spectroscopy with an Avatar 360 spectrometer from Nicolet. The conversion rates were calculated from the disappearance of the vinyl C=C stretching vibration band at 1410 cm^{-1}.

The absorption measurements were performed using an Evolution 220 Thermo Scientific UV-Vis spectrometer.

Transmission electron microscopy (TEM) was used to characterize the size and shape of silver nanoparticles. The samples were irradiated directly onto the copper grid. TEM measurements were carried out using a Philips CM20 instrument with LaB_6 cathode.

Results and discussions

The key step of the process is the reaction of silver cations with photogenerated species that are able to both reduce them to silver metal atoms (nanoparticles) and initiate the polymerization of the host medium. For this, it was used the direct homolytic photocleavage of a sigma bond from 2-hydroxy-4' -2-(hydroxy-ethoxy)-2-methyl-propiophenone (Irgacure 2959) to generate radicals, which induce the formation of silver nanoparticles at the same time with the polymerization of acrylic reactive oligomer. The formation of silver nanoparticles during the polymerization was confirmed by UV-Vis absorption (the color of the samples turned to brown-yellow) (fig. 1).

Transmission electron microscopy analysis of the samples indicated the formation of polydisperse spherical nanoparticles with diameters in the 3 - 22 nanometer range (fig. 2). Sample P2 - 0.2% $AgNO_3$, contains nanoparticles with the diameter between 4 and 6 nm, but there are also present a small number of nanoparticles with the diameter between 12 and 18 nm. Sample P3 - 0.5% $AgNO_3$, displayed nanoparticles with a diameter between 3 and 5 nm, but also nanoparticles with diameter between 10 and 17 nm. Sample P4 - 1% $AgNO_3$ is comprised of nanoparticles with the diameter between 9 and 14 nm and also nanoparticles with diameter of 20 nm. Sample P5 - 2% $AgNO_3$ consists of nanoparticles with a diameter between 3 and 5 nm, but also some nanoparticles with a diameter of 10 nm.

This bimodal nanoparticles size distribution can be explained by the long process initiation period which results in the formation of an unbalance between the nucleation and growth rate (fig. 3) [22].

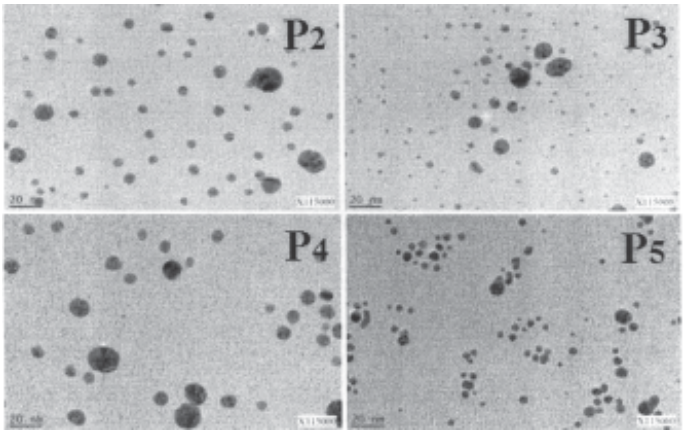

Fig. 2. TEM analysis of obtained nanoparticles using different concentrations of $AgNO_3$ (%wt): P2 (0.2%), P3 (0.5%), P4 (1%), P5 (2%) and 0.5% (%wt) Irgacure 2959

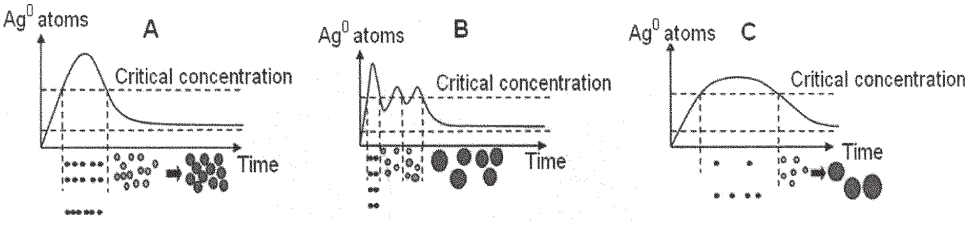

Fig. 3. Nucleation and growth schemes: A- Optimized experimental conditions: nucleation and growth equilibrium; B - multistep nucleation due to nucleation rate too high or initiation time too long; C – nucleation rate too low [22]

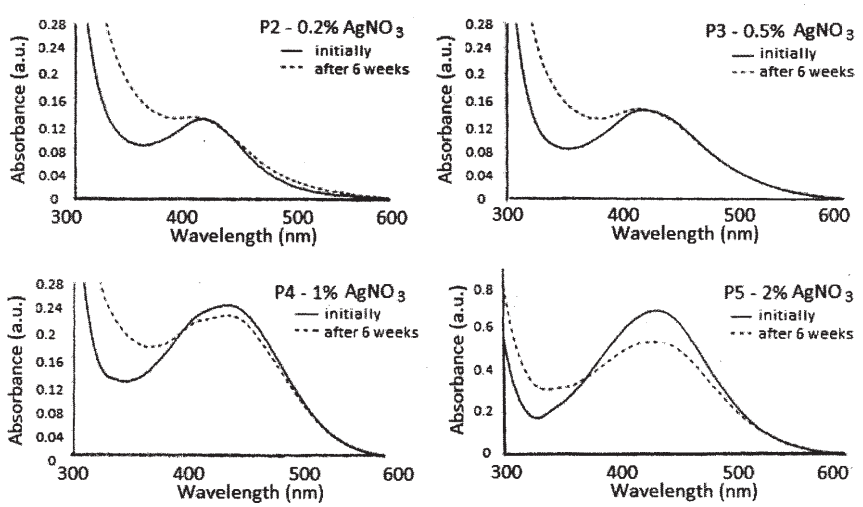

Fig. 4. Stability over time of the obtained samples (Photoinitiator: 0.5% (wt) Irgacure 2959; Lamp intensity: 50%; Irradiation time: 110 min)

UV-visible spectra of all samples were recorded after irradiation (110 min at 50% lamp intensity) and after 6 weeks, in order to show the stability (fig. 4).

A fair stability of the samples even after 6 weeks illumination was noticed (fig. 4). Increasing the concentration of Ag decreases the stability of the samples. At the highest concentration, stability is poor, which means the concentration of the nanoparticles is sufficient to cause their coalescence with time. The maximum absorption for each sample has a narrow domain of variation.

Influence of the irradiation time and lamp intensity on the formation of nanoparticles

The Ag NP formation by irradiation at intensity of 10% of the lamp is quite slow and there is a critical threshold of 120 minutes; below 120 min , the absorbance is almost constant; between 120 and 240 min there is a significant increase in the absorbance and beyond 240 min the absorbance is again almost constant. At low irradiation intensities (10%) the rate of silver is low, which results in a decreased supersaturation level, a reduced particle number (lower absorption) with an increase in particle size (higher wavelength) (fig. 3C). The nanoparticles formation rate is much lower than the polymerization rate. Over a long time interval, a complete polymerization is achieved and the nanoparticle synthesis decreases and runs out in the end.

Regarding the wavelength, the values vary in a narrow domain which indicates that the nanoparticles are formed with the same size throughout the entire process (fig. 5).

When increasing the intensity of the lamp at 50%, absorbance constantly increases in the first 120 min and then stabilizes, meaning the number of nanoparticles increases steadily for the first 120 min after which the formation process is complete. The wavelength is found to diminish with increasing the irradiation time, which means that the diameter of the nanoparticles decreases slightly.

At the maximum irradiation intensity, the polymerization rate is very high resulting in a complete polymerization process before silver ions reduction and nanoparticles formation takes place. For these reasons the highest absorbance were recorded for irradiation intensities of 50%. The best conditions for obtaining silver nanoparticles-polymer composites corresponded to a molar ratio $AgNO_3$/ Photoinitiator close to 1 and the irradiation intensity was adjusted so that the polymerization and nanoparticles formation rates were of the same order (fig. 5). The optimum irradiation time was 110 min with an irradiation intensity of 50%.

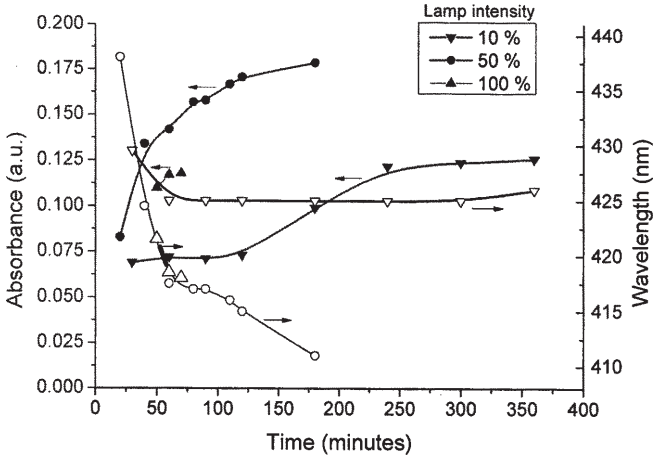

Fig. 5. Time evolution of absorbance (solid symbols) and wavelength (open symbols) for different lamp intensities (Silver precursor: 0.2% (wt) $AgNO_3$; Photoinitiator: 0.5% (wt) Irgacure 2959)

Influence of the $AgNO_3$ concentration on the formation of nanoparticles

The absorbance is directly proportional to the amount of silver in the sample. However there is also a bathochromic shift of the maximum absorption when increasing the amount of silver in the sample; this is due to the formation of nanoparticles with larger diameter (fig. 6).

The polymerization of the acrylate resin was followed by real-time Fourier transformed infrared spectroscopy, by monitoring the disappearance of the characteristic band of the acrylate double bonds: 1410 cm^{-1} (fig. 7).

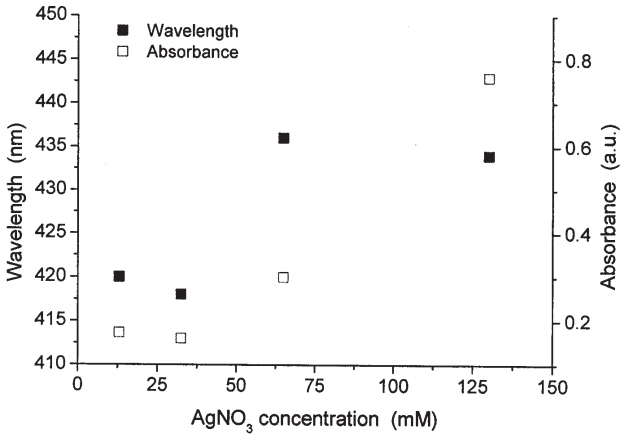

Fig 6. Influence of $AgNO_3$ concentration on the absorbance and wavelength (Photoinitiator: 0.5% Irgacure 2959; Lamp intensity: 50%; Irradiation time: 110 min)

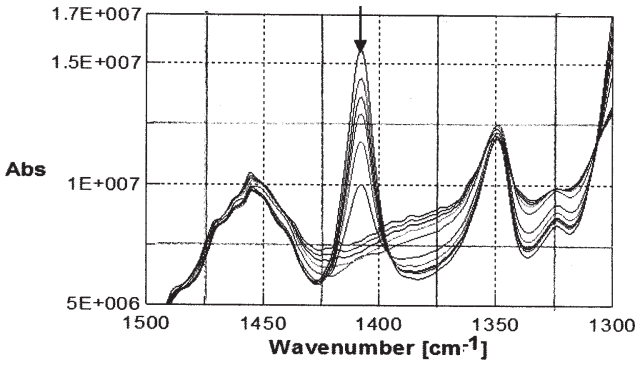

Fig. 7. Real-time FT-IR spectra of sample containing 0.5% (wt) $AgNO_3$ and 0.5% (wt) photoinitiator Irgacure 2959

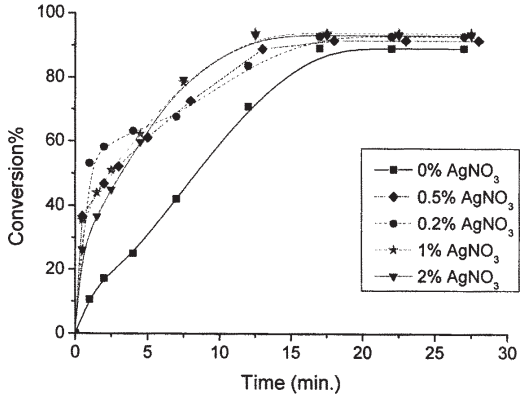

Fig. 8. Conversion of double bond acrylate monomer (Photoinitiator: 0.5% (wt) Irgacure 2959; Lamp intensity: 50%)

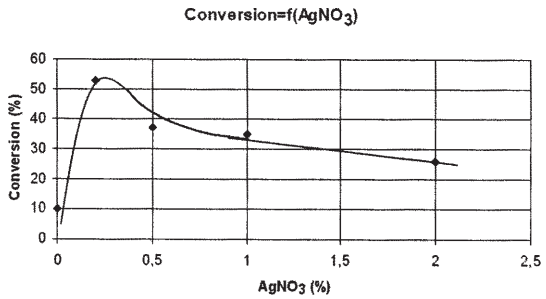

Fig. 9. The conversion dependence versus $AgNO_3$ concentration for the first minute of polymerization

Table 1
CORRELATION BETWEEN THE MOLAR RATIO AGNO3/IRGACURE 2959 AND RELATIVE ABSORBANCE, OLIGOMER CONVERSION AFTER 1 MINUTE AND POLYMERIZATION RATE AT AN IRRADIATION INTENSITY OF 50%.

Sample	Molar ratio $AgNO_3$/Irgacure 2959	Absorbance (a.u) / [$AgNO_3$]	Oligomer conversion at 1 min.	Polymerization rate
P2	0.95/1	10	53	↑
P3	1.3/1	4.66	37	
P4	2.6/1	4	35	
P5	5.8/1	5.83	26	

The conversion of monomer into polymer is influenced by the formation of silver nanoparticles. For the blank sample (without $AgNO_3$) the monomer conversion occurs gradually; after the first minute of irradiation it is only 10%. For the samples containing silver precursor, the conversion of the monomer into polymer is much faster ; after one minute, it is 26% for the sample with 2% $AgNO_3$, 35% with 1% $AgNO_3$, 37% with 0.5% $AgNO_3$ and 53% with 0.2% $AgNO_3$. The ultimate conversion degree was of about 90% for all the samples containing silver nitrate (fig. 8).

In figure 9 is represented the dependence of the conversion registered after 1 min versus $AgNO_3$ concentration.

The analysis of figure 9 reveals that the polymerization rate in the presence of the $AgNO_3$ increased up to a critical value, after which it decreased with the increase of $AgNO_3$ concentration. Nevertheless, it remains at higher rate value than the blank experiment, in the absence of $AgNO_3$.These results sustain the similar behaviour observed in a previous study [23].

The higher polymerization rate can be explained by an increase of the radicals concentration. The numbers of the radicals generated in the system can be correlated with the molar ratio $AgNO_3$/Irgacure 2959. The highest value was obtained for the sample P2 at almost equimolecular ratio. The increase of molar ratio between the two components results in a decrease of polymerization rate (table 1).

In the case of samples 2 and 3, the ratio $AgNO_3$/ Photoinitiator is close to 1, the viscosity of the solution increases at the same time with the silver nanoparticles generation, thus the higher polymerization rate present in sample 2 can explain the narrower size distribution for this system.

In the case of samples 4 and 5, the ratio $AgNO_3$/ Photoinitiator is higher than 1, which entails that there are not sufficient ketyl radicals formed to reduce all the silver ions resulting in a decrease of nanoparticle size and number (decrease of relative absorbance). In this case part of the silver nanoparticles is obtained by direct photolysis process of the silver nitrate.

Conclusions

A silver–acrylate nanocomposite was prepared using a novel one-pot strategy involving simultaneous photoinduced reduction and free radical polymerization processes.

Silver nanoparticles were characterized by UV-visible in order to show the stability in time and the influence of several factors (lamp intensity, irradiation time and silver nitrate concentration) on formation of nanoparticles.

TEM analysis was used in order to establish the shape and size of nanoparticles. Spherical nanoparticles with diameters in the 3 up to 22 nanometer range were obtained.

The conversion was above 90% for all the samples.

The optimum conditions for obtaining the silver-polymer nanocomposites have been determined (silver precursor

concentration, molar ratio silver precursor/photoinitiator, irradiation time and intensity).

Acknowledgment:The work has been funded by the Sectoral Operational Programme Human Resources Development 2007-2013 of the Romanian Ministry of Labour, Family and Social Protection through the Financial Agreement POSDRU/107/1.5/S/76909.

References

1.BALAN L., SCHNEIDER R., LOUGNOT D., J. Prog. Org. Coat., **62**, 2008, p.351.
2. KRÓL-GRACZ A., MICHALAK E., NOWAK P., DYONIZY A., Cent. Eur. J. Chem., **9**, 2011, p. 982.
3. CHOI S. H., ZHANG Y. P., GOPALAN A., LEE K. P., KANG H. D., Colloids Surf. A., **256**, 2005, p.165.
4. AL-GHAMDI H. S., MAHMOUD W. E., Mater. Lett., **105**, 2013, p.62.
5. QIN Y., JI X., JING J., LIU H., WU H., YANG W., Colloids Surf. A, **372**, 2010, p.172.
6. ZAMIRI R., ZAKARIA A., AHANGAR H. A., SADROLHOSSEINI A. R., MAHDI M. A., Int. J. Mol. Sci., **11**, 2010, p.4764.
7. ZAMIRI R., AZMI B. Z., SADROLHOSSEINI A. R., AHANGAR H. A., ZAIDAN A. W., MAHDI M. A., Int. J. Nanomed., **6**, 2011, p.71.
8. HORIKOSHI S., ABE H., TORIGOE K., ABE M., SERPONE N., Nanoscale, **2**, 2010, p.1441.
9. WANG B., ZHUANG X., DENG W., CHENG B., Engineering, **2**, 2010, p.387.
10. KRISHNARAJ C., JAGAN E. G., RAJASEKAR S., SELVAKUMAR P., KALAICHELVAN P. T., MOHAN N., Colloids Surf. B: Biointerfaces, **76**, 2010, p.50.
11.SARKAR A., MUKHERJEE T., KAPOOR S., Res. Chem. Intermed., **36**, 2010, p.173.
12. TALEBI J., HALLADJ R., ASKARI S., J. Mat. S., **45**, 2010, p.3318.
13. KUTSENKO A. S., GRANCHAK V. M., Theor. Exp. Chem., **45**, 2009, p.313.
14. ZHENG X., ZHAO X., GUO D., TANG B., XU S., ZHAO B., XU W., LOMBARDI J. R., Langmuir, **25**, 2009, p.3802.
15. SAKAMOTO M., FUJISTUKA M., MAJIMA T., J. Photochem. Photobiol. C, **10**, 2009, p.33.
16. BALAN L., SCHNEIDER R., TURCK C., LOUGNOT D., MORLET-SAVARY F., J. Nanomat., **1**, 2012, p.1.
17. BALAN L., MALVAL J. P., SCHNEIDER R., LE NOUEN D., LOUGNOT D., J. Polym., **51**, 2010, p.1363.
18. BALAN L., MALVAL J. P., SCHNEIDER R., BURGET D., Mater. Chem. Phys., **104**, 2007, p.417.
19. NICOLAIS L., CAROTENUTO G., Metal-Polymer Nanocomposites, Wiley, 2004.
20. BALAN L., BURGET D., Eur. Polym. J., **42**, 2006, p.3180.
21. POREL S., SINGH S., HARSHA S. S., RAO D. N., RADHAKRISHNAN T. P., Chem. Mater., **17**, 2004, p.9.
22. BLOSI M., ALBONETTI S., DONDI M., MARTELLI C., BALDI G., J. Nanopart. Res., **13**, 2011, p.127.
23. CHIOLERIO A., VESCOVO L., SANGERMANO M., Macromol. Chem. Phys., **211**, 2010, p.18

Manuscript received: 13.01.2014